Mechanism of the Addition Half of the *O*-Acetylserine Sulfhydrylase-A Reaction†

Wael M. Rabeh, Susan S. Alguindigue, and Paul F. Cook*

Department of Chemistry and Biochemistry, University of Oklahoma, 620 Parrington Oval, Norman, Oklahoma 73019

Received December 1, 2004; Revised Manuscript Received January 24, 2005

ABSTRACT: *O*-Acetylserine sulfhydrylase (OASS) catalyzes the last step in the cysteine biosynthetic pathway in enteric bacteria and plants, substitution of the β-acetoxy group of *O*-acetyl-L-serine (OAS) with inorganic bisulfide. The first half of the sulfhydrylase reaction, formation of the α-aminoacrylate intermediate, limits the overall reaction rate, while in the second half-reaction, with bisulfide as the substrate, chemistry is thought to be diffusion-limited. In order to characterize the second half-reaction, the pH dependence of the pseudo-first-order rate constant for disappearance of the α-aminoacrylate intermediate was measured over the pH range 6.0−9.5 using the natural substrate bisulfide, and a number of nucleophilic analogues. The rate is pH-dependent for substrates with a pK_a > 7, while the rate constant is pH-independent for substrates with a pK_a < 7 suggesting that the pK_as of the substrate and an enzyme group are important in this half of the reaction. In D_2O, at low pD values, the amino acid external Schiff base is trapped, while in H_2O the reaction proceeds through release of the amino acid product, which is likely rate-limiting for all nucleophilic reactants. A number of new β-substituted amino acids were produced and characterized by ^{1}H NMR spectroscopy.

O-Acetylserine sulfhydrylase (OASS) catalyzes the PLP-dependent replacement of the β-acetoxy of OAS[1] by inorganic bisulfide to produce L-cysteine (*1*). Ultraviolet−visible spectral studies are consistent with an internal Schiff base (λ_{max} = 412 nm) present as the resting form of OASS-A, with the α-aminoacrylate external Schiff base (λ_{max} = 330, 470 nm) present after elimination of the β-acetoxy group (*2*−*5*). OASS-A has a ping-pong Bi Bi kinetic mechanism with competitive inhibition by both substrates resulting from substrates binding to an allosteric anion binding site (*6*). The three-dimensional structure of the 68900 Da OASS-A dimer has been solved to 2.2 Å resolution (*7*). Each subunit is composed of N- and C-terminal domains with one active site located deep within the protein at the interface between the two domains. The PLP cofactor, located at the bottom of the active site cleft, is in Schiff base linkage with the ϵ-amino group of Lys-41 (*8*).

The first half of the OASS-A reaction starts with binding and nucleophilic attack of the monoanionic form of the amino acid substrate, OAS, on the imine of the internal Schiff base to form the external Schiff base, Scheme 1. α,β-Elimination then produces the stable α-aminoacrylate intermediate and acetate is released. The V/K_{OAS} pH profile, which reflects the conversion of the internal Schiff base of the enzyme and OAS to the α-aminoacrylate intermediate, shows a pK_a of about 7 on the acid side for an enzyme group that must be protonated for optimum catalysis. It is thought that this group is involved in the conformational changes the protein undergoes as the reaction proceeds (*9*). The α-amine of the amino acid substrate must be unprotonated to facilitate its nucleophilic attack on C4′ of PLP, which results in a rapid shift in the λ_{max} from 412 nm (the internal Schiff base) to 418 nm (OAS external Schiff base) with a rate constant of about 800 s^{-1} (*10*). In the second half-reaction with β-chloro-L-alanine (BCA) and 5-thio-2-nitrobenzoate (TNB) as substrates, pK_a values of 6.9 and 7.4 are observed in the V/K_{BCA} profile, with the pK_a of 6.9 identical to the one observed in the V/K_{OAS} profile and the pK_a of 7.4 reflecting the α-amine of BCA (*11*). No quinonoid (Q) intermediate was observed under the conditions used. The absence of Q in the reverse of the first half-reaction even in the presence of D_2O, which slows down the protonation at C_α, is consistent with an E2 reaction (*9*, *12*). The first half-reaction limits the overall reaction with rate constant of 280 s^{-1}, similar to the turnover number of the enzyme in which the slow step is the α-proton abstraction and the β-elimination of acetate yields the α-aminoacrylate intermediate (*13*).

The second half-reaction of OASS-A is, formally, the reversal of the first half-reaction with the nucleophilic substrate, bisulfide, adding to C_β of the α-aminoacrylate intermediate to form the external Schiff base with cysteine. The amino acid product is then released after transimination. The second half-reaction is very fast with a first-order rate constant >1000 s^{-1} measured with 5 μM bisulfide at pH 6.5 (*14*). As a result, the nucleophilic substrate is thought to diffuse into the active site and form the product upon

† This work was supported by the Grayce B. Kerr endowment to the University of Oklahoma to support the research of P.F.C.

* Author to whom correspondence should be addressed. Tel: 405-325-4581. Fax: 405-325-7182. E-mail: pcook@chemdept.chem.ou.edu.

[1] Abbreviations: AA, α-aminoacrylate external Schiff base intermediate; BCA, β-chloro-L-alanine; Caps, 3-(cyclohexylamino)-1-propanesulfonic acid; Ches, 2-(*N*-cyclohexylamino)ethanesulfonic acid; DTNB, 5,5′-dithiobis(2-nitrobenzoate); DTT, dithiothreitol; E, internal Schiff base; ESB(I), OAS external Schiff base; ESB(II), cysteine external Schiff base; GD, *geminal*-diamine intermediate; Hepes, *N*-(2-hydroxyethyl)piperazine-*N*′-2-ethanesulfonic acid; Mes, 2-(*N*-morpholino)ethanesulfonic acid; OAS, *O*-acetyl-L-serine; OASS-A, the A-isozyme of *O*-acetylserine sulfhydrylase; PLP, pyridoxal 5′-phosphate; RSSF, rapid-scanning stopped flow; Taps, 3-[tris(hydroxymethyl)-methylamino]propanesulfonic acid; TNB, 5-thio-2-nitrobenzoate.

10.1021/bi047479i CCC: $30.25
Published on Web 03/18/2005

Scheme 1: Proposed Chemical Mechanism for OASS-A[a]

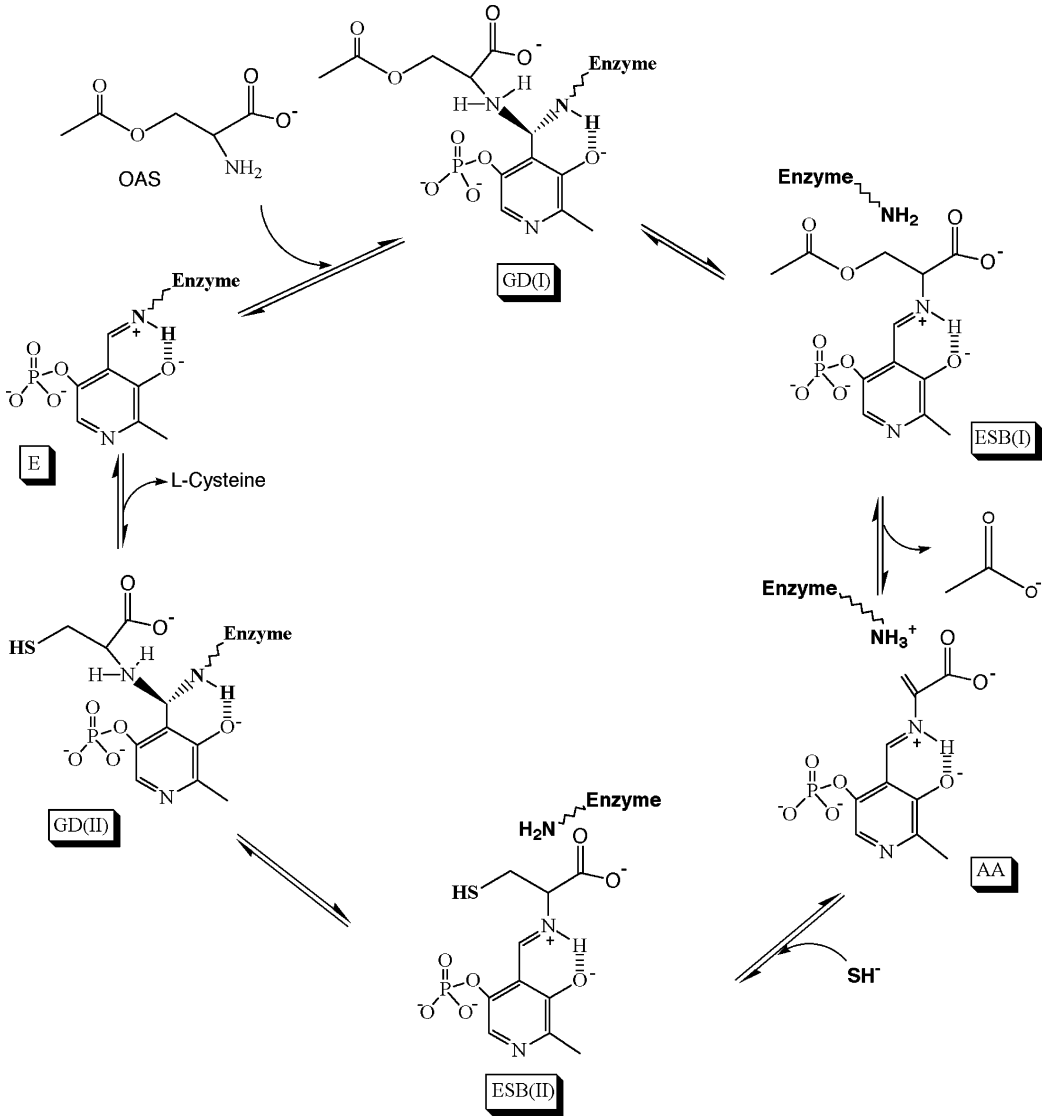

[a] E: the internal Schiff Base. GD(I): *geminal*-diamine intermediate. ESB(I): OAS external Schiff base. AA: the α-aminoacrylate intermediate. ESB(II): cysteine external Schiff base. GD(II): *geminal*-diamine intermediate with cysteine.

collision. In agreement with this suggestion, no binding site for bisulfide has been observed in the OASS-A active site (*15*). The pH dependence of the *V*/*K* for TNB (an alternative substrate) when BCA is used as the amino acid substrate shows pK_a values of 6.9 and 8.3, with these pK_as reflecting the pH-dependent conformational change and the Schiff base lysine (Lys-41) that must protonate C_α of the α-aminoacrylate intermediate to form the product external Schiff base (*11*).

The rate of the second half-reaction is at or very near the diffusion limit, and as a result, limited information is available on the second half-reaction of OASS-A. In this study, rapid-scanning-stopped-flow (RSSF) experiments are used in an attempt to detect intermediates along the reaction pathway in the addition half-reaction. The pH(D) dependence of the second half-reaction has been determined using the natural substrate, bisulfide, and sulfide analogues. Data are discussed in terms of the overall mechanism of OASS-A.

MATERIALS AND METHODS

Chemicals and Enzyme. 2-Mercaptoethanol, mercaptosuccinic acid, 2-mercaptopyridine, thiosalicylic acid, mercaptoacetic acid, and cyanide were obtained from Aldrich Chemicals, while 1,2,4-triazole, *O*-acetyl-L-serine, 5,5′-dithiobis(2-nitrobenzoic acid), and formic acid were obtained from Sigma. Phenol was from Fisher scientific, and buffers (Ches, Hepes, Tris, and Taps) were from Research Organics. All other chemicals and reagents were obtained from commercial sources and were of the highest purity available. *O*-Acetylserine sulfhydrylase-A (OASS-A) was purified from a plasmid-containing overproducing strain using the method of Hara et al. (*16*) adapted to HPLC (*17*).

Enzyme Assay. The activity of OASS-A was monitored using 5-thio-2-nitrobenzate (TNB) as the nucleophilic substrate (*17*). TNB was prepared fresh daily by the reduction of 5,5′-dithiobis(2-nitrobenzoate) (DTNB) with dithiothreitol (DTT). The disappearance of TNB was monitored continually at 412 nm (ϵ_{412}, 13600 M^{-1} cm^{-1}) using a Beckman DU 640 spectrophotometer and a circulating water bath to maintain the temperature of the cell compartment at 25 °C. All assays were carried out in 100 mM Hepes, pH 7.0, at 25 °C with an OAS concentration of 1 mM and a TNB concentration of 50 μM.

Rapid-Scanning Stopped Flow. Pre-steady-state kinetic measurements were carried out using an OLIS-RSM 1000 stopped-flow spectrophotometer in the multiple wavelength mode. Sample solutions were prepared in two syringes at the same pH with a final buffer concentration of 100 mM. The first syringe contained enzyme at a final concentration no lower than 15 μM, and enough OAS was added to convert the free enzyme to the α-aminoacrylate intermediate. The second syringe contained sulfide or a sulfide analogue at twice the desired final concentration. Data were collected with a repetitive scan rate of 15 ms for the wavelength range 280−600 nm, and the number of scans collected was dependent on the rate of the reaction. The disappearance of the α-aminoacrylate external Schiff base was monitored at 470 and 330 nm, and the appearance of the internal Schiff base was monitored at 412 nm. The reaction temperature was maintained at 25 °C using a circulating water bath. At 25 °C, the pH was varied from 5.0 to 6.5 for sulfide, fixed at 7.0 for 2-mercaptoethanol, mercaptosuccinic acid, 2-mercaptopyridine, phenol, hydroxylamine, and formate, and varied from 5.5 to 8 for thiosalicylate, mercaptoacetate, 1,2,4-triazole, and cyanide. The pH was measured at the beginning and end of the reaction, and the following buffers were used for the pH ranges indicated: Mes (pH 5.0−6.5), Hepes (pH 7.0−8.0), and Taps (pH 8.5−9.5). Experiments were also carried out at 8, 15, and 35 °C.

The rapid-scanning stopped-flow (RSSF) spectral data were fitted using the software provided by OLIS. To obtain the first-order rate constant (k_{obs}) for the conversion of the α-aminoacrylate intermediate to free enzyme, eq 1 was used.

$$A_t = A_0\, e^{(-k_{obs}t)} + B_0 \quad (1)$$

In eq 1, A_t is the absorbance at any time t, A_0 is the absorbance at time zero, and B_0 corrects for the background absorbance. The first-order rate constants (k_{obs}) obtained at different nucleophile concentrations were fitted to the equation for a straight line, which gave the slope as the second-order rate constant, k_{max}/K_s, eq 2.

$$k_{obs} = \frac{k_{max}}{K_s}[\text{nucleophile}] \quad (2)$$

The second-order rate constant was measured at different pH values, and the resulting data were fitted to eq 3 with a BASIC version of a FORTRAN program developed by Cleland (*18*).

$$\log y = \log \frac{C}{1 + K/H} \quad (3)$$

In eq 3, y is the observed value of k_{max}/K_s at any pH, C is the pH-independent value of y, H is the hydrogen ion concentration, and K is the acid dissociation constant of a group on enzyme. The second-order rate constant was plotted vs reciprocal temperature at pH 7.0, and the enthalpy of activation was estimated graphically according to eq 4.

$$\log(k_{max}/K_s) = -\frac{E_{act}}{2.303R}\left(\frac{1}{T}\right) \quad (4)$$

In eq 4, E_{act} is the energy of activation of the reaction and T is the absolute temperature in K.

Stopped-Flow Solvent Isotope Effect Studies. The pD dependence of the second half of the OASS-A reaction was measured using cyanide, 1,2,4-triazole, and mercaptoacetate as nucleophilic substrates. All buffers and substrates were prepared in D_2O, and the pD value was adjusted with DCl or KOD as needed. The pD value was measured using a pH meter, which was previously equilibrated in D_2O for 30 min. The pD value was calculated by adding 0.4 to the pH meter reading to correct for the isotope effect on the pH electrode (*19*). The OASS-A stock solution was exchanged into D_2O by concentrating the enzyme to about 0.1 mL using an Amicon ultrafiltration cell. The enzyme was diluted with 5 mL of buffer in D_2O, concentrated to 0.1 mL, and diluted with 1 mL of buffer in D_2O. Sample solutions were prepared in two syringes at the same pD value with a final buffer concentration of 100 mM as described above. Experiments were then carried out at 25 °C and 8 °C. The pD value for each reaction mixture was obtained before and after each run in which the pD change during the reaction was not significant. The RSSF spectra were collected, and data at 412 nm and 470 nm were fitted using eqs 1 and 2 as described above. The pD profile was obtained by plotting the second-order rate constant vs pD.

Ultraviolet−Visible Spectral Studies. Absorbance spectra of the *O*-thioacetyl-L-serine external Schiff base of OASS-A were recorded utilizing a Hewlett-Packard 8452A photodiode array spectrophotometer over the wavelength range 300−600 nm. The temperature was maintained at 25 °C in a reaction cuvette of 1 cm path length and 1 mL volume at pD 6.0 using 100 mM Mes. The blank contained all components minus enzyme. The α-aminoacrylate intermediate was generated by adding OAS equal to the enzyme concentration. Mercaptoacetate was added to a final concentration of 10 mM to yield the *O*-thioacetyl-L-serine external Schiff base.

NMR Spectroscopy. A number of amino acids were prepared using 10 mM OAS, 10 mM nucleophile, and 0.5 mg of OASS-A. All substrates and enzyme were prepared in D_2O as described above, and the pD value of the reaction mixture was maintained at 6.5 using 100 mM phosphate buffer. The enzyme was added last to initiate the reaction, and the reaction mixture was incubated at room temperature overnight. The structural identity of the products was confirmed using NMR, and spectra were collected on a Varian Mercury VX-300 MHz NMR spectrometer. The spectra were referenced to the residual HDO peak at 4.69 ppm. The proton spectra were collected using a presaturation pulse sequence to minimize the water peak with an acquisition time of 2 s and 16 scans. The carbon spectra were collected in 10000 scans with a delay of 1 s. Assignment of NMR resonances employed an atom numbering system starting with C_α of the amino acid substrate. Assignments of ^1H and ^{13}C NMR resonances were confirmed by two-dimensional spectroscopy (COSY). The gCOSY sequence supplied by Varian was employed with 128 increments and 1 transient. Data for the amino acids studied are as follow.

O-Acetyl-L-serine. ^1H NMR (D_2O, 300 MHz) gave δ 4.34 (m, 2H, C(β)-H_2), 3.92 (M, 1H, C(α)-H_1) 1.97 (CH_3). ^{13}C NMR (D_2O, 75 MHz) gave δ 171.5, 171.6 (C = 0), 63.1 (C(β)), 53.5 (C(α)), 19.5 (CH_3).

S-2-Pyridyl-L-cysteine. ^1H NMR (D_2O, 300 MHz) gave δ 8.22 (ddd, 1H, J = 5.1, 1.5, 1.0 Hz C(6)-H), 7.50 (m, 1H,

C(4)-H), 7.24 (dt, 1H, $J = 8.3, 1, 1$, C(β)-H), 7.04 (ddd, 1H, $J = 8.0, 5.0, 1.0$ Hz, C(5)-H), 3.58 (d, 1H, $J = 15$ Hz, C(β)-H_2), 3.33 (d, 1H, $J = 15$ Hz, C(β)-H_2).

*S-2-Hydroxyethyl-*L*-cysteine.* ^{1}H NMR (D_2O, 300 MHz) gave δ 3.6 (td, 2H, $J = 6.0, 1.1$ Hz, C(ϵ)-H_2), 2.96 (m, 2H, C(β)-H_2), 2.61 (t, 2H, $J = 6.0$ Hz, C(d)-H_2).

*β-1,2,4-Triazole-*L*-alanine.* ^{1}H NMR (D_2O, 300 MHz) gave δ 8.32, 7.93 (s,2H, C(3)-H, C(5)-H), 4.5 (m, 2H, C(β)-H).

*β-Cyano-*L*-alanine.* ^{1}H NMR (D_2O, 300 MHz) gave δ 2.86 (d, 2H, $J = 6.0$ Hz, C(β)-H). ^{13}C NMR (D_2O, 75 MHz) gave δ 173.6 (C═O), 117.6 (CN), 50.3 (C(α)), 20.41 (C(β)).

A time course was obtained for the cyanide reaction using the above presaturation pulse sequence with a variable preacquisition delay time and eight scans averaged per data point. Forty-one data points were collected over a period of 16 h. These points were collected every 250 s in the first hour, every 900 s for the next 3 h, and one point each hour for the last 12 h. It was possible to monitor the reaction using both the increase of the β-cyano-L-alanine product C(β)-H_2 (2.86 ppm) and the appearance of acetate (1.77 ppm) versus time. The time dependence of the acetate resonance was fitted to eq 5.

$$[\text{acetate}] = a\, e^{-kt} \quad (5)$$

RESULTS

Rapid-Scanning Stopped-Flow Studies. RSSF measurements were carried out to obtain information on the identity and the rate of appearance and disappearance of intermediates in the pre steady state for the second half of the OASS-A reaction. The α-aminoacrylate intermediate exhibits maxima at 330 and 470 nm (*10*). The intermediate was preformed in one syringe and reacted with different concentrations of sulfide or sulfide analogues in the second syringe. Reaction with sulfide gives a rapid disappearance of the α-aminoacrylate intermediate and appearance of free enzyme (λ_{max}, 412 nm) within the RSSF instrument dead time of about 4 ms (data not shown). Only at pH 5.0 with a total sulfide concentration of 1.5 μM was the last portion of the time course for disappearance at 470 nm observed, with a pseudo-first-order rate constant of $\sim$100 s^{-1} estimated.

Since the rate of the second half-reaction was too fast to measure with the natural substrate, bisulfide, attempts were made to monitor the reaction using nucleophilic analogues of sulfide. Different nucleophiles containing sulfur, nitrogen, carbon, or oxygen were tested as possible substrates, Table 1. Reaction of all nucleophiles shown in Table 1 was conducted at pH 7.0. The nucleophiles are split into classes depending on the functional group. The rate of disappearance of the α-aminoacrylate intermediate was measured as a function of nucleophile concentration using the stopped-flow method by monitoring the reaction at 412 and 470 nm. As an example, data obtained with 1,2,4-triazole are shown in Figure 1. The spectral time course exhibits two clear isosbestic points, which suggests that the two tautomeric forms of the α-aminoacrylate intermediate, maxima at 470 and 330 nm, are converted to the internal Schiff base, λ_{max} at 412 nm, with no detectable accumulation of additional intermediates. The time courses for the increase in absorbance at 412 nm and the decrease in absorbance at 470 nm give identical rate constants, Figure 1B, as expected for interconversion of two species. The first-order rate constant (k_{obs}) obtained using the RSSF method at different nucleophile concentrations is a linear function of analogue concentration, and its slope represents the second-order rate constant (k_{max}/K_s), Figure 2. A summary of data obtained for a variety of nucleophilic substrates is given in Table 1. In addition to the nucleophiles listed, others that gave no detectable reaction are thiophenol, 2-mercaptoimidazole, 2-mercaptobenzoxazole, pyridine, *m*-bromophenol, benzoin, benzimidazole, benzoate, 4-nitrothiophenol, 4-chlorophenol, 2-mercaptobenzimidazole, and 2-chloroaniline.

^{1}H NMR Spectroscopy. To confirm the structure of the amino acid product obtained from the reaction of OASS-A with different sulfide analogues, spectra were measured using ^{1}H NMR. Figure 3A shows an example of NMR spectra for the reaction of OASS-A with 10 mM OAS and 10 mM cyanide at pD 6.5 as a function of time. Spectra were obtained at time zero, before any enzyme was added, and then as a function of time. The time course for production of acetate was fitted to eq 5 to yield a first-order rate of 0.0076 min^{-1}. From Figure 3B, the following assignments are made: the 1.77 ppm resonance is due to the CH_3 of the product acetate, the 1.97 ppm resonance is due to the CH_3 of the acetoxy group of OAS, the 2.86 ppm resonance is due to C_β of β-cyano-L-alanine (the amino acid product), the 3.92 ppm resonance is due to C_α of OAS, and the 4.34 ppm resonance is due to C_β of OAS. β-Cyano-L-alanine would also have a resonance at 3.78 ppm due to C_α, but this position is deuterated in the product as a result of carrying out the reaction in D_2O. The 4.34 ppm resonance of the C_β of OAS is shifted to 2.86 ppm as a result of replacement of the acetoxy group of OAS by a cyanide group in the β-cyano-L-alanine product. The 1.97 ppm resonance of the CH_3 of OAS is shifted to 1.91 ppm in acetate. The spectrum of the final product of this reaction agrees with the spectrum obtained with the commercially available β-cyano-L-alanine.

The structure of the different amino acid products was identified using NMR spectroscopy. This was especially helpful when an analogue contained more than one potential nucleophile. An example is the reaction of the α-aminoacrylate intermediate with mercaptoethanol, where the nucleophilic group could be either its oxygen or thiol group. The proton chemical shifts for the amino acid substrate, OAS, were significantly different from those of the amino acid product, as a result of the electron deshielding effects of the surrounding nuclei (*20*). The ^{1}H NMR spectrum of the amino acid product, *S*-2-hydroxyethyl-L-cysteine, shows that the β-protons (2.96 ppm) are shifted upfield (toward 0.0 ppm) from its position of 4.34 ppm in the OAS spectrum. Oxygen is more electronegative than sulfur and pulls electrons away from the β-protons causing a significantly larger chemical shift value in OAS compared to the amino acid products. If oxygen was the attacking group, the β-protons of the amino acid product would have been located between 3.6 and 4.5 ppm (*20*).

pH Dependence of the Second-Order Rate Constant. To further investigate whether functional groups on enzyme and/or nucleophilic substrate are involved in catalysis, the second-order rate constant (k_{max}/K_s) was measured as a function of pH using several of the nucleophiles including cyanide, 1,2,4-triazole, mercaptoacetate, and thiosalicylate. The second-order rate constant was measured at 25 °C over the pH range

Table 1: Kinetic Data for Nucleophilic Substrate Analogues

Nucleophilic Substrate	$(k_{max}/K_s)^a$ (M^{-1} s^{-1})	$(k_{max}/K_s)^b$ (M^{-1} s^{-1})	pK_a	Product Analog
Carboxyl				
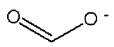 Formic acid	$(8 \pm 4)X10^{-3}$	NC	3.6	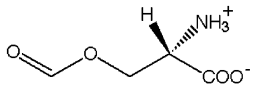 *O*-formyl-L-serine
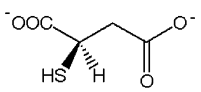 2-mercaptosuccinate	1.25 ± 0.25	NC	4.4	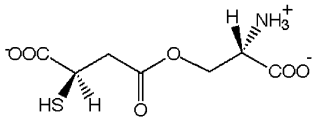 *O*-3-*R*-mercaptosuccinyl-L-serine
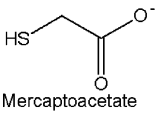 Mercaptoacetate	7.1 ± 0.3	NC	3.5	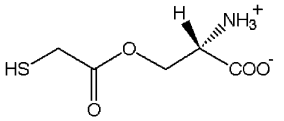 *O*-mercaptoacetyl-L-serine
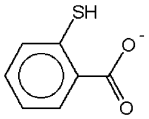 Thiosalicylate	510 ± 70	NC	4.0	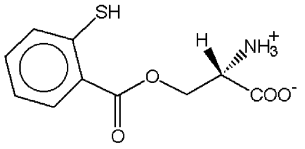 *O*-2-mercaptobenzoyl-L-serine
Hydroxyl				
H_2N—OH Hydroxylamine	0.11 ± 0.04	NC	6.0	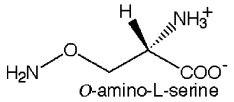 *O*-amino-L-serine
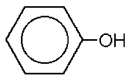 Phenol	$(1.4 \pm 0.2) X10^{-3}$	$(9 \pm 1) X10^{3}$	9.8	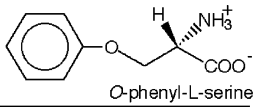 *O*-phenyl-L-serine
Thiol				
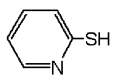 2-mercaptopyridine	$(1.1 \pm 0.1) X10^{-2}$	$(1.1 \pm 0.1) X10^{4}$	10	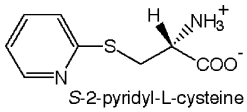 *S*-2-pyridyl-L-cysteine
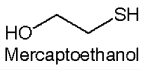 Mercaptoethanol	1.00 ± 0.04	$(2.5 \pm 0.1) X10^{5}$	9.4	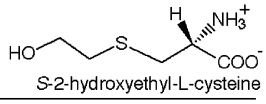 *S*-2-hydroxyethyl-L-cysteine
Others				
$N\equiv C^-$ Cyanide	0.21 ± 0.03	$(2.9 \pm 0.4) X10^{4}$	9.1	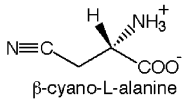 β-cyano-L-alanine
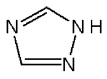 1,2,4-triazole	$(6.5 \pm 0.5) X10^{-2}$	$(6.5 \pm 0.5) X10^{4}$	10	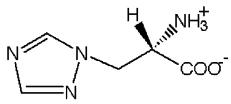 β-1,2,4-triazole-L-alanine

[a] Rate measured at pH 7. [b] pH-independent rate. NC, no correction of the rate.

5.5−8.0. Data were not collected above pH 8.0 because of the high rate of decomposition of the α-aminoacrylate intermediate to free enzyme, ammonia, and pyruvate (*3*). In the case of mercaptoacetate, Figure 4, and thiosalicylate (data not shown), the second-order rate constant is pH-independent. On the other hand, the pH dependence of the second-order rate constants at 25 °C measured with cyanide, Figure 5B, and 1,2,4-triazole (not shown) were qualitatively very similar with a limiting slope of +1 and an apparent pK_a of 7.2 ± 0.2 for both substrates.

To decrease the rate of decomposition of the α-aminoacrylate intermediate, the second-order rate constants for cyanide and 1,2,4-triazole were measured at 8 °C. Thus, data could be collected at pH values higher than 7.5. The pH dependence of the second-order rate constants for cyanide, Figure 5C, and 1,2,4-triazole (not shown) at 8 °C are similar with a limiting slope of +1. A pK_a value of 8.1 ± 0.7 was observed in both pH profiles.

The pH dependence of the second-order rate constant for the second half of the OASS-A reaction was also measured with cyanide at 15 and 35 °C, Figure 5A, and gave a limiting slope of +1 with pK_a values of 7.2 ± 0.2 and 7.6 ± 0.7, respectively. An Arrhenius plot, Figure 6, of data at pH 7 is nonlinear with a transition at around 18 °C. Heats of activation were calculated using the limiting slopes of the curve in Figure 6 at low and high temperature, respectively,

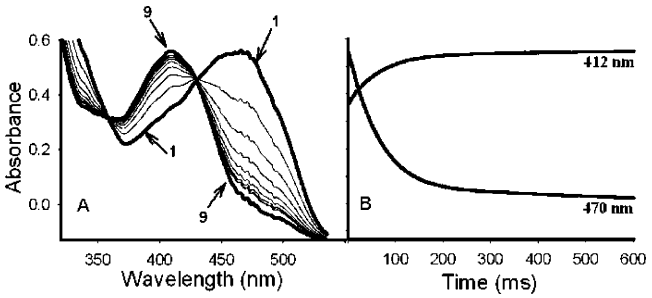

FIGURE 1: Rapid-scanning stopped-flow spectra of the conversion of the α-aminoacrylate intermediate of OASS-A to free enzyme using 1,2,4-triazole as the nucleophilic substrate. (A) Spectrum 1 represents the α-aminoacrylate intermediate with λ_{max} at 470 and 330 nm, and spectrum 9 represents free enzyme (internal Schiff base) with λ_{max} at 412 nm. The time interval between spectra is about 13 s. The enzyme concentration was 80 μM, and 1,2,4-triazole was 1 mM. Data were measured at pH 6.0, 100 mM Mes, and 25 °C. (B) Time courses obtained from data in Figure 1A at 412 and 470 nm. The rate constant calculated from both wavelengths is identical. No other intermediates are detected under these conditions.

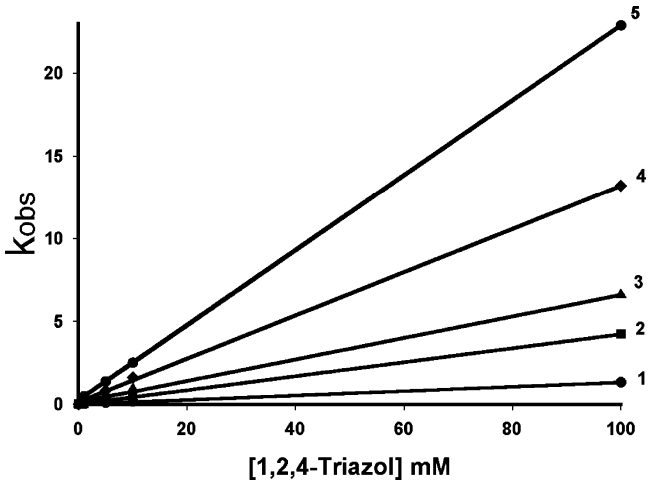

FIGURE 2: Plot of the observed first-order rate constant for the second half of the OASS-A reaction (measured as in Figure 1) against the concentration of 1,2,4-triazole. All data were collected at 25 °C, and pH values of 6.0, 6.5, 7.0, 7.5, and 8.0 represent lines 1−5, respectively. The second-order rate constant (k_{max}/K_s) is the slope of the line, and was calculated using eq 2.

according to eq 4. The energy of activation at temperatures >18 °C is about 10.2 kJ/mol but increases approximately 17-fold at temperatures <18 °C (E_{act} = 170 kJ /mol).

Spectral Studies in D_2O. If protonation of C_α in the second half of the OASS-A reaction to give the external Schiff base, ESB(II), is rate-limiting, a solvent kinetic deuterium isotope effect is predicted. All RSSF spectra obtained in D_2O exhibit two clear isosbestic points, similar to those shown in water, Figure 1. However, the enzyme spectrum obtained after the reaction of the nucleophilic substrate with the α-aminoacrylate intermediate in D_2O has a λ_{max} of 418 nm compared to that of the free enzyme in D_2O, λ_{max} at 412 nm. The reaction of mercaptoacetate with the α-aminoacrylate intermediate in D_2O thus yields the *O*-mercaptoacetyl-L-serine external Schiff base form of the enzyme, Figure 7A, where spectrum 1 is the absorbance spectrum of the α-aminoacrylate intermediate obtained in D_2O and spectra 2 and 3 are the absorbance spectra of the *O*-mercaptoacetyl-L-serine external Schiff base at pD 6.0 (λ_{max}, 418 nm) and 7.9 (λ_{max}, 412 and 418 nm), respectively. At pD 7.9, the *O*-mercaptoacetyl-L-serine external Schiff base spectrum suggests an equilibrium between the free and the external Schiff base forms of the enzyme. Addition of 1 mM OAS to the enzyme with a λ_{max} at 418 nm gives the α-aminoacrylate intermediate, which was detected at 470 nm. On the basis of the above, the final enzyme form obtained upon the reaction of different nucleophiles with the α-aminoacrylate intermediate in D_2O is the product external Schiff base, as opposed to that of the internal Schiff base in H_2O. To determine whether the external Schiff base formed in D_2O is stable, its spectrum was recorded using a photodiode array spectrophotometer as described in the Materials and Methods section. In Figure 7B, spectrum 1 is the absorbance spectrum for free enzyme measured at pD 6.0, and spectrum 2 is the absorbance spectrum for *O*-mercaptoacetyl-L-serine external Schiff base at pD 6.0. There is no shift in the λ_{max} of free enzyme in D_2O compared to H_2O.

Stopped-Flow Solvent Isotope Effect Studies. In order to determine whether a solvent deuterium isotope effect is observed, the pD dependence of the second-order rate constant was measured as above using cyanide, 1,2,4-triazole, and mercaptoacetate. The second-order rate constant at 25 °C, using mercaptoacetate, is pD-independent (Figure 4) and yields an inverse solvent isotope effect with a $^{D_2O}(k_{max}/K_s)$ of about 0.2. The second-order rate constant is pD-dependent over the pD range 6.0−8.5 measured at 25 °C with cyanide, Figure 5B, and 1,2,4-triazole (not shown), which exhibit a slope of +1 with a pK_a value of 7.9 ± 0.7. The data in D_2O nearly superimpose on the data obtained in H_2O, in spite of the shift to a higher pD value observed as a result of the equilibrium isotope effect on the pK_a of the group titrated (*19*). The pD profile obtained for both substrates has large errors at pD higher than 8.0. As a result, the value of the solvent isotope effect was not calculated but is inverse and near 0.4, on the basis of the expected shift in the pK_a (see above). The pD dependence of the second-order rate constant for cyanide and 1,2,4-triazole were also measured at 8 °C to lower the rate of the α-aminoacrylate intermediate decomposition. The pD profile obtained at 8 °C for cyanide (Figure 5C) and that obtained for 1,2,4-triazole (not shown) are similar with a limiting slope of +1, and superimpose on the data obtained in H_2O. A pK_a value of 8.9 ± 0.7 was obtained from the pD profile for cyanide. An inverse solvent isotope effect with $^{D_2O}(k_{max}/K_s)$ of about 0.45 was calculated from the pH(D) cyanide profiles.

DISCUSSION

Rapid-Scanning Stopped-Flow Studies. Very little is known about the second half of the OASS-A reaction in which the α-aminoacrylate intermediate and bisulfide, the true substrate for the enzyme, are converted to L-cysteine and free enzyme. Previous studies indicated the second half-reaction to be very rapid, and the only species observed upon reacting enzyme with OAS and bisulfide are the α-aminoacrylate intermediate and free enzyme (*10*). It was thus proposed that the second half-reaction is diffusion limited. In agreement, the $V/K_{sulfide}E_t$ is 8×10^7 M^{-1} s^{-1} (*11*). In the present studies, the only condition that allowed a measurable pre-steady-state rate of disappearance of the α-aminoacrylate intermediate, 100 s^{-1}, was obtained with a total sulfide concentration of 1.5 μM at pH 5.0. Sulfide has two pK_a

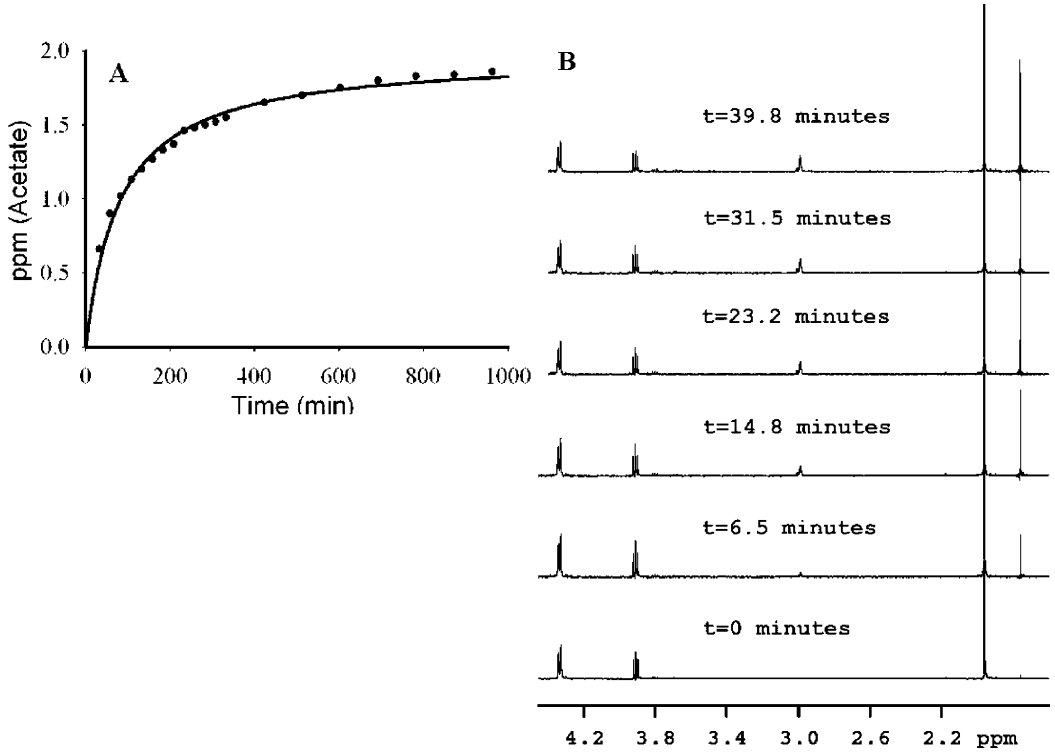

FIGURE 3: ^{1}H NMR spectra of the OASS-A catalyzed reaction using 10 mM OAS and 10 mM cyanide at pD 6.5, 100 mM phosphate buffer as described in Materials and Methods. All spectra were referenced to the residual HDO peak at 4.69 ppm. (A) Time course obtained using cyanide as the nucleophilic substrate. A presaturation pulse sequence was used with a variable preacquisition delay time and eight scans per data point. Forty-one data points were collected over a period of 16 h. These points were collected every 250 s in the first hour, every 900 s for the next 3 h, and one point each hour for the last 12 h. It was possible to monitor the reaction using the appearance of acetate (1.77 ppm) versus time with a first-order rate constant of 0.0076 min^{-1}. (B) NMR spectra collected at the beginning of the reaction ($t = 0$) before adding any enzyme and at different time intervals as labeled on the spectra. At $t = 0$, the ^{1}H NMR spectrum is identical to the OAS spectrum in which its ^{1}H NMR (D_2O, 300 MHz) gave δ 4.34 (m, 2H, C(β)-H_2), 3.92 (M, 1H, C(α)-H_1), and 1.97 (CH_3). The final spectrum of the reaction mixture is identical to that of β-cyano-L-alanine in which its ^{1}H NMR (D_2O, 300 MHz) gave δ 2.86 (d, 2H, $J = 6.0$ Hz, C(β)-H). The α-proton is not observed since the position is deuterated as a result of the reaction being run in D_2O.

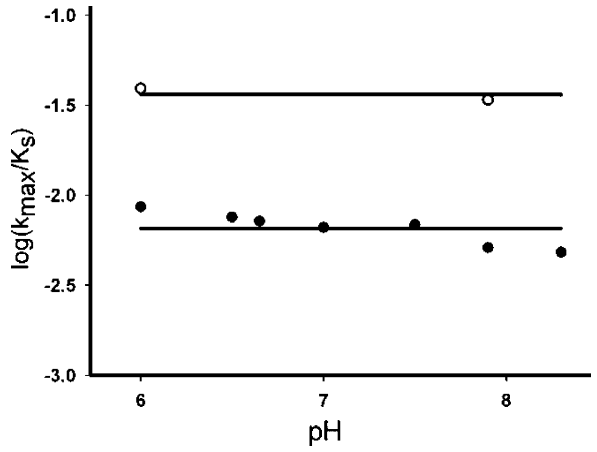

FIGURE 4: pH (●) and pD (○) dependence of the second-order rate constant measured with mercaptoacetate at 25 °C as described in Materials and Methods. Points are experimental values, and the line is the average value. Inverse solvent deuterium isotope effect is observed with a $^{D_2O}(k_{max}/K_s)$ value of about 0.2.

values, 6.8 and 13.8, so that at pH 5.0 most of the sulfide is H_2S, and bisulfide, the true substrate for OASS-A, is only 24 nM.

In an attempt to slow down the second half-reaction, a number of nucleophiles were used as analogues of the second substrate, bisulfide. For all the nucleophiles tested, no nucleophile was found to have a second-order rate constant equal to that obtained with bisulfide. On the other hand, one can relate nucleophilicity of the analogues to their pK_a values, Table 1. Nucleophiles with low pK_a values have a lower second-order rate-constant (k_{max}/K_s) when compared to those with high pK_a values, in agreement with the proposed direct nucleophilic attack of the nucleophile on the α-aminoacrylate intermediate. In Table 1, nucleophiles from the carboxyl class show that size does not play a major role in determining the rate of the second half-reaction. However, nucleophiles from the carboxyl class have a lower second-order rate constant than all other classes because they have a lower nucleophilicity. Nonetheless, as demonstrated in Table 1, the high turnover number for OASS-A, along with its acceptance of a wide variety of nucleophilic substrates, makes it a good tool for the preparation of a number of new β-substituted α-amino acids, even when the rate constant is low.

pH Dependence of the Second-Order Rate Constant. Enzyme kinetic parameters and/or microscopic rate constants are a function of pH because of ionization of protic positions on the enzyme and/or substrate. In a ping-pong kinetic mechanism, the V/K pH profile for the substrates reflects the individual half-reactions (*21*). The V/K_{TNB} pH profile obtained with BCA as the amino acid substrate yields pK_a values of about 7 on the acid side and 8.2 on the basic side (*11*). The enzyme group with a pK_a of 7 must be unprotonated to stabilize the optimum catalytic conformation of the enzyme, while the enzyme group with a pK_a of 8.2 is attributed to the ϵ-amino group of Lys-41, which must be protonated to donate a proton to C_α of the α-aminoacrylate

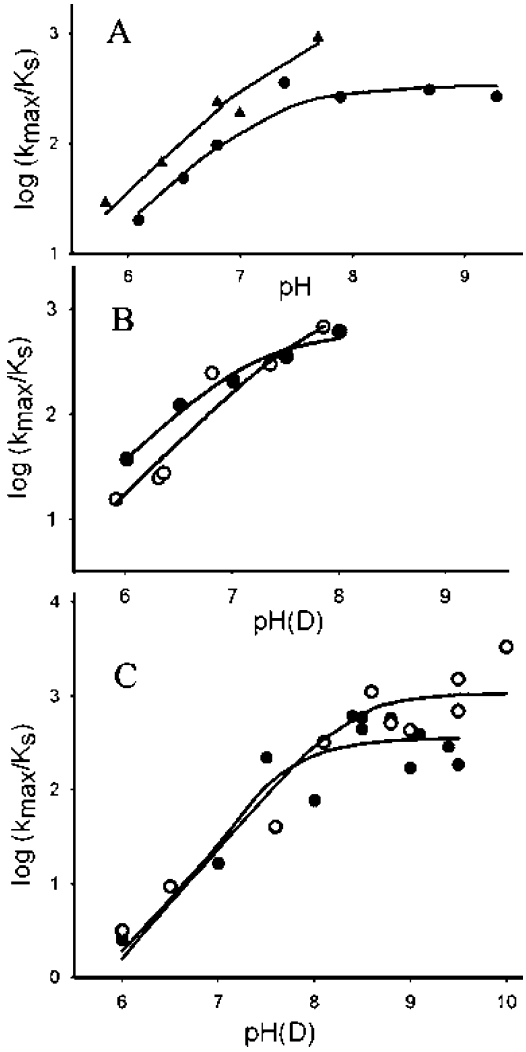

FIGURE 5: pH(D) dependence of the second-order rate constant measured with cyanide. (A) The pH dependence of the second-order rate constant collected at (●) 15 °C and (▲) 35 °C gave pK_a values of 7.2 ± 0.2 and 7.6 ± 0.7, respectively. (B) The pH(D) dependence of the second-order rate constant collected at 25 °C in (●) H_2O and (○) D_2O gave pK_a values of 7.2 ± 0.2 and 7.9 ± 0.7, respectively. (C) The pH(D) dependence of the second-order rate constant collected at 8 °C in (●) H_2O and (○) D_2O gave pK_a values of 8.1 ± 0.7 and 8.9 ± 0.7, respectively. An inverse solvent isotope effect was observed at all temperatures tested with a calculated $^{D_2O}(k_{max}/K_s)$ value of about 0.45 at 8 °C. The rate data were fitted using eq 3. Points are experimental values, and the curve is theoretical based on the fit to eq 3.

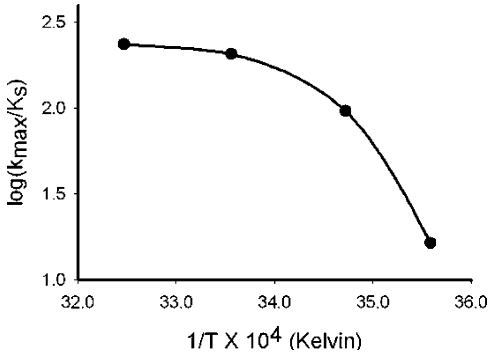

FIGURE 6: Arrhenius plot of the second-order rate-constant of the second half-reaction of OASS-A at pH 7. The Arrhenius plot obtained shows a biphasic pattern, with a transition at around 18 °C. The E_{act} value was calculated from the graph giving values at temperature >18 °C of 10.2 kJ/mol and 170 kJ /mol at temperatures <18 °C.

intermediate as the amino acid external Schiff base, ESB-(II), is formed, Scheme 1.

In the pre steady state, k_{max}/K_s for the sulfide analogues reflects the slow step(s) in the conversion of the α-aminoacrylate intermediate and sulfide analogue to free enzyme and amino acid product. In this study, the pH profiles for thiosalicylate and mercaptoacetate at 25 °C are pH-independent. Both nucleophiles have low pK_a values of 4.0 and 3.5, respectively. The pH independence of k_{max}/K_s indicates that neither enzyme nor substrate functional groups are titrated over the pH range 5.5−8.0. In both cases, the pK_a of the nucleophile is not observed because it is lower than pH 5.5.

The behavior of nucleophiles with high pK_a values is different. The pH−rate profiles at 25 °C for cyanide (Figure 5B) and 1,2,4-trizole (not shown) are pH-dependent with the requirement for a group on the acid side with a pK_a of about 7, while cyanide and 1,2,4-triazole have pK_a values of 9.1 and 10, respectively. If the pH−rate profiles could be extended to high enough pH, one would expect k_{max}/K_s to decrease above the pK_a of the nucleophile. Data suggest that reverse protonation states exist between the nucleophile and the enzyme group with a pK_a of 7, so that although the group with a pK_a of 7 is observed on the acid side of the proifile, it is required protonated, while the nucleophile, although required unprotonated, would be observed on the basic side of the profile. At 35 °C, Figure 5A, although the pH range is again limited, data are similar to those obtained at 25 °C. Data at 15 °C, Figure 5A, however, indicate a pH-independent region above 7.5 to about 9, in agreement with the above explanation; a pK_a of about 7.6 is now observed on the acid side of the profile.

As discussed above, the group with a pK_a of 7 must be protonated, opposite to the interpretation based on the pH dependence of the steady-state parameter V/K_{TNB}. In the steady state the starting point is the α-aminoacrylate external Schiff base and free TNB, and the group with a pK_a of 7 must be unprotonated to stabilize the closed conformation (*11*). In the pre steady state the slow step is the conformational change to open the active site and release product, and the group with a pK_a of 7 must be protonated to stabilize the open conformation.

At 8 °C, a condition that exhibits a large E_a at pH 7, a higher pK_a is observed in the log(k_{max}/K_{CN}) vs pH profile. The pK_a is near 8, 0.5 pH unit higher than that observed at the higher temperatures. In addition, the rate appears to be decreasing above pH 9, consistent with the pK_a of cyanide. The plot of log(k_{max}/K_{CN}) at pH 7 vs $1/T$ is biphasic, suggesting a change in rate-limiting step with a break at about 18 °C. Data support a rate-limiting conformational change accompanying product release requiring an enzyme group with a pK_a of 7 protonated, as suggested above. This is likely true for all substrates including bisulfide. At lower temperature, however, the conformational change is very slow.

pD Dependence of the Absorbance Spectra. In H_2O, the enzyme form present after reaction of the α-aminoacrylate intermediate with nucleophile is the internal Schiff base (free enzyme, E). In D_2O using cyanide, 1,2,4-triazole, or mercaptoacetate as the nucleophilic substrate, the amino acid external Schiff base (ESB(II), λ_{max} 418 nm) is the final form

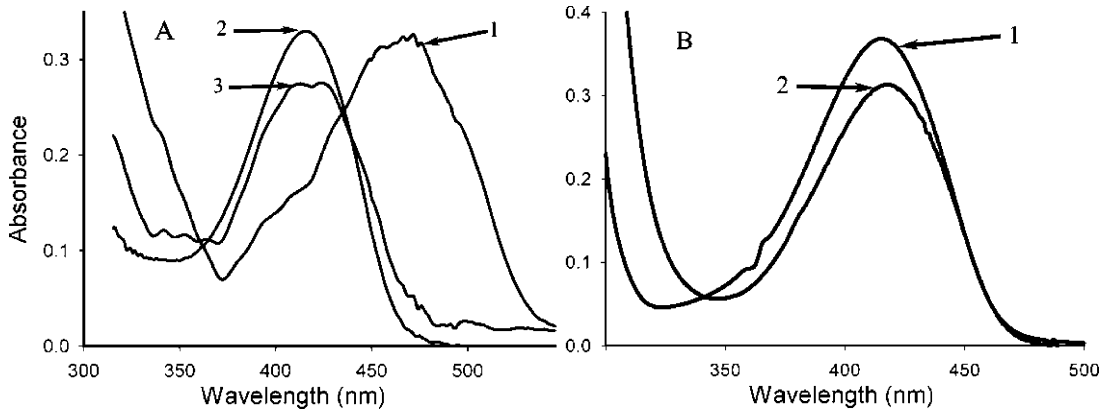

FIGURE 7: (A) RSSF spectra for the reaction of the α-aminoacrylate intermediate with 10 mM mercaptoacetate in D_2O. Plot 1 is the absorbance spectrum of the starting complex, the α-aminoacrylate intermediate; plots 2 and 3 are the absorbance spectra of the *O*-mercaptoacetyl-L-serine external Schiff base at pD 6.0 (λ_{max} at 418 nm) and 7.9 (λ_{max} at 412 and 418 nm), respectively. (B) UV−visible spectra collected using photodiode array spectrophotometer at pD 6.0. Plot 1 is the absorbance spectrum of free OASS-A, and plot 2 is the *O*-mercaptoacetyl-L-serine external Schiff base measured in D_2O.

of the enzyme at pD 6.0, Figure 7. Reaction of the α-aminoacrylate intermediate (AA) with different concentrations of the nucleophilic substrate in D_2O gave the ESB(II) without releasing the amino acid product, while free enzyme (λ_{max} 412 nm) is present at the end of the reaction in H_2O. Data indicate that the conformational change to open the active site is very slow in D_2O. At pD 7.9, the second half-reaction in D_2O yields an equilibrium between the ESB(II) and the free enzyme forms, Scheme 1. Thus the pH and pD profiles cannot be directly compared to give a solvent deuterium isotope effect. In D_2O, product release does not occur in the time scale of the assay and thus a large inverse solvent deuterium isotope effect is observed, suggesting the involvement of a group on the protein to open the active site, consistent with the above discussion. The observed pD-independent rate is faster in D_2O than the pH-independent rate in H_2O as a result of the very slow conformational change in D_2O, k_2 in Scheme 2.

Scheme 2

$$AA + SH^- \xrightarrow{k_1} ESB \xrightarrow{k_2} E + L\text{-}Cys$$

The Chemical Mechanism of the OASS-A Reaction. The amino acid substrate, OAS, binds as the monoanionic form with its α-amine unprotonated to carry out a nucleophilic attack on C4′ of the internal Schiff base (E). As the OAS external Schiff base (ESB(I), observed transiently in the pre steady state with OAS as the substrate (*10*)) is formed via *geminal*-diamine intermediates, GD(I), the active site closes triggered by the interaction of the substrate α-carboxylate with the asparagine loop (*22*). Lys-41, initially in internal Schiff base linkage with PLP, serves as a general base to deprotonate C_α in the α,*β*-elimination reaction responsible for the release of acetate and the formation of the α-aminoacrylate intermediate (AA) to end the first half of the OASS-A reaction. The active site opens partially to release the first product, acetate, and allow entry of bisulfide, the second nucleophilic substrate. The difference in conformation of the external Schiff base and the α-aminoacrylate external Schiff base forms of the enzyme is clearly shown by differences in their ^{31}P NMR chemical shifts (*23*).

At the beginning of the second half-reaction, Lys-41 is protonated and the nucleophilic substrate diffuses into the active site and attacks C_β of the AA to give ESB(II). The nucleophile has no binding site as a substrate and likely adds to the AA directly upon diffusion into the active site (*10*). The ESB(II) is formed upon addition of the nucleophile to the AA as was indicated by the shift in the λ_{max} from 412 to 418 nm upon adding cysteine to OASS-A in the reverse direction of the second half-reaction (*5*). The ESB(II) is rapidly formed and does not accumulate in the pre steady state but is seen transiently when cysteine adds to free enzyme to form the cysteine external Schiff base (*10*). A *geminal*-diamine intermediate, GD(II), is expected to precede ESB(II), where the ϵ-amino group of Lys-41 and the amino acid product are bonded to C4′ of PLP. No *geminal*-diamine intermediate was visualized under the experimental conditions used in this study, and the addition of cysteine to free enzyme in the pre steady state also does not show the presence of a *geminal*-diamine intermediate (*10*). The presence of one or more *geminal*-diamine intermediates is important to release the amino acid products, thus the formation and decay of GD(II) must be very rapid, and the equilibrium between this intermediate and the free enzyme must be far toward the latter. The active site then opens to expel the cysteine product upon transimination by Lys-41. This step requires an enzyme group with a pK_a of 7.0 to be protonated to open the active site as was observed in the k_{max}/K_s pH profile for cyanide and 1,2,4-triazole. No quinonoid intermediate was detected in the second half of the OASS-A reaction under the experimental conditions used. Data are in agreement with the absence of a quinonoid intermediate in the first half of the OASS-A reaction under all the experimental conditions used (*5*, *10*). The chemical step, represented by the proton transfer step, is not rate limiting; rather, the enzyme conformational change to open the active site and release the amino acid substrate is the rate-limiting step in the second half-reaction. The second half-reaction in D_2O yields the ESB(II) form of the enzyme, which is the locked conformation as a result of the requirement for a proton transfer step to open the active site and release the amino acid product. On the other hand, at pD 7.9, the enzyme ESB(II) complex was found in equilibrium with the free enzyme form (E) as a result of having the enzyme group that is important to open the active site, unprotonated.

In conclusion, the second half of the OASS-A reaction is limited by the conformational change needed to open the active site and release the amino acid product, and this appears to be true in the case of all nucleophilic reactants including bisulfide. No quinonoid or *geminal*-diamine intermediates were detected; rather, the amino acid external Schiff base of the enzyme was found to be very stable when the reaction was run in D_2O.

REFERENCES

1. Becker, M. A., Kredich, N. M., and Tomkins, G. M. (1969) The Purification and Characterization of *O*-Acetylserine Sulfhydrylase-A from *Salmonella typhimirium*. *J. Biol. Chem. 244*, 2418−2427.
2. Cook, P. F., and Wedding, R. T. (1976) A Reaction Mechanism from Steady-State Kinetic Studies for *O*-Acetylserine Sulfhydrylase from *Salmonella typhimurium* LT-2. *J. Biol. Chem. 251*, 2023−2029.
3. Cook, P. F., Hara, S., Nalabolu, S., and Schnackerz, K. D. (1992) pH dependence of the absorbance and ^{31}P NMR spectra of *O*-acetylserine sulfhydrylase in the absence and presence of *O*-acetyl-L-serine. *Biochemistry 31*, 2299−2303.
4. Cook, P. F., Tai, C.-H., Hwang, C.-C., Woehl, E. U., Dunn, M. F., and Schanckerz, K. D. (1996) Substitution of Pyridoxal 5′-Phosphate in the *O*-Acetylserine Sulfhydrylase from *Salmonella typhimurium* by Cofactor Analogs Provides a Test of the Mechanism Proposed for Formation of the α-Aminoacrylate Intermediate. *J. Biol. Chem. 271*, 25842−25849.
5. Schnackerz, K. D., Tai, C.-H., Simmons, J. W., III, Jacobson, T. M., Rao, G. S. J., and Cook, P. F. (1995) Identification and Spectral Characterization of the External Aldimine of the *O*-Acetylserine Sulfhydrylase Reaction. *Biochemistry 34*, 12152−12160.
6. Tai, C.-H., Burkhard, P., Gani, D., Jenn, T., Johnson, C., and Cook, P. F. (2001) Characterization of the Allosteric Anion-Binding Site of *O*-Acetylsrine Sulfhydrylase. *Biochemistry 40*, 7446−7452.
7. Burkhard, P., Rao, G. S. J., Hoehenester, E., Schnackerz, K. D., Cook, P. F., and Jansonius, J. N. (1998) Three-Dimensional Structure of *O*-Acetylserine Sulfhydrylase from *Salmonella typhimurium*. *J. Mol. Biol. 283*, 121−133.
8. Rege, V. D., Kredich, N. M., Tai, C.-H., Karsten, W. E., and Cook, P. F. (1995) Role of Lysine 42 in the β-Elimination Reaction Catalyzed by *O*-Acetylserine Sulfhydrylase A from *Salmonella typhimurium*. *FASEB J. 9*, A1297.
9. Tai, C.-H., and Cook, P. F. (2001) Pyridoxal 5′-Phosphate-Dependent α,β-Elimination Reactions: Mechanism of *O*-Acetylserine Sulfhydrylase. *Acc. Chem. Res. 34*, 49−59.
10. Woehl, E. U., Tai, C.-H., Dunn, M. F., and Cook, P. F. (1996) Formation of the α-Aminoacrylate Intermediate Limits the Overall Reaction Catalyzed by *O*-Acetylserine Sulfhydrylase. *Biochemistry 35*, 4776−4783.
11. Tai, C.-H., Nalabolu, S. R., Simmons, J. W., III, Jacobson, T. M., and Cook, P. F. (1995) Acid−Base Chemical Mechanism of *O*-Acetylserine Sulfhydrylases-A and -B from pH Studies. *Biochemistry 34*, 12311−12322.
12. Karsten, W. E., Tai, C.-H., and Cook, P. F. (2002) Detection of Intermediates in the Reactions Catalyzed by PLP-Dependent Enzymes. *Methods Enzymol. 354*, 223−237.
13. Tai, C.-H., Nalabolu, S. R., Jacobson, T. M., Minter, D. E., and Cook, P. F. (1993) Kinetic Mechanisms of the A and B Isozymes of *O*-Acetylserine Sulfhydrylases from *Salmonella typhimurium* LT-2 Using the Natual and Alternative Reactants. *Biochemistry 32*, 6433−6442.
14. Hwang, C.-C., Woehl, E. U., Dunn, M. F., and Cook, P. F. (1996) Kinetic Isotope Effects as a Probe of the β-Elimination Reaction Catalyzed by *O*-Acetylserine Sulfhydrylase. *Biochemistry 35*, 6358−6365.
15. Burkhard, P., Tai, C.-H., Jansonius, J. N., and Cook, P. F. (2000) Identification of an Allosteric Anion-Binding Site on *O*-Acetylserine Sulfhydrylase: Structure of the Enzyme with Chloride Bound. *J. Mol. Biol. 303*, 279−286.
16. Hara, S., Payne, M. A., Schnackarz, K. D., and Cook, P. F. (1990) A Rapid Purification Procedure and Computer-Assisted Sulfide Ion Selective Electrode Assay from *O*-Acetylserine Sulfhydrylase from *Salmonella typhimurium*. *Protein Expression Purif. 1*, 70−76.
17. Tai, C.-H., Nalabolu, S. R., Jacobson, T. M., Minter, D. E., and Cook, P. F. (1993) Kinetic mechanisms of A and B isozymes of *O*-acetylserine sulfhydrylase from *Salmonella typhimurium* LT-2 using the natural and alternative reactants. *Biochemistry 32*, 6433−6442.
18. Cleland, W. W. (1979) Statistical Analysis of Enzyme Kinetic Data. *Methods Enzymol. 63*, 103−138.
19. Schowen, K. B., and Schowen, R. L. (1982) Solvent isotope effects on enzyme systems, in *Solvent isotope effects on enzyme systems*, Academic Press, Inc., New York.
20. Silverstein, R. M., and Webster, F. X. (1998) *Spectrometric Identification of Organic Compounds*, 6th ed., Wiley, New York.
21. Cleland, W. W. (1977) Determining the chemical mechanisms of enzyme-catalyzed reactions by kinetic studies. *Adv. Enzymol. 45*, 273−387.
22. Burkhard, P., Tai, C.-H., Ristroph, C., Cook, P. F., and Jansonius, J. N. (1999) Ligand Binding Induces a Large Conformational Change in *O*-Acetylserine Sulfhydrylase from *Salmonella typhimurium*. *J. Mol. Biol. 291*, 941−953.
23. Tai, C.-H., Cook, P. F., and Schnackerz, K. D. (2000) Conformation of the α-Aminoacrylate Intermediate of *O*-Acetylserine Sulfhydrylase from *Salmonella typhimurium* as Inferred from ^{31}P NMR Spectroscopy. *Protein Pept. Lett. 7*, 207−210.

BI047479I